Blood snoRNAs and miRNAs as predictors of COVID-19 Severity

Aijaz Parray
Hamad Medical Corporation
Fayaz Mir
Hamad Medical Corporation
Asmma Doudin
Community College of Qatar
Ahmad Iskandarani
Hamad Medical Corporation
Ibn Mohammed Danjuma
Hamad Medical Corporation
Rahim Kuni
Hamad Medical Corporation
Alaaedin Abdelmajid
Hamad Medical Corporation
Ibrahim Abdelhafez
Qatar University
Rida Arif
Qatar University
Mohammad Mulhim
Hamad Medical Corporation
Mohammad Abukhattab
Hamad Medical Corporation
Shoukat Dar
Hamad Medical Corporation
Eyad Elkord
Hamad Bin Khalifa University
Abdul Latif Al-khal
Hamad Medical Corporation
Abdel-Naser Elzouki
Hamad Medical Corporation
Farhan Cyprian (farhan.cyprian@gmail.com)
Qatar University

Article

Keywords: COVID-19, non-coding RNAs, severity

Posted Date: July 7th, 2021

DOI: https://doi.org/10.21203/rs.3.rs-679490/v1

Abstract

There is a lack of predictive markers for early and rapid identification of disease progression in COVID-19 patients. Our study aims at identifying non-coding RNAs (ncRNAs) as potential biomarkers of COVID-19 severity. Using differential expression analysis of microarray data (n = 29), we identified hsa-miR-494-3p, hsa-miR-1246, ACA40, hsa-miR-4532, ACA15 as the top five differentially expressed transcripts in severe versus asymptomatic, and ACA40, hsa-miR-3609, hsa-miR-6790-5p, hsa-miR-126-3p, hsa-miR-885-3p as the most significant five in severe versus mild cases. Moreover, we found that WBC count, absolute neutrophil count, neutrophil (%), lymphocyte (%), RBC count, hemoglobin, hematocrit, D-Dimer and albumin were significantly correlated with the identified ncRNAs. Altogether, we present the first comprehensive analysis of COVID-19-associated microRNA (miRNA)/ small nucleolar RNA (snoRNA) signature, highlighting the importance of ncRNAs in SARS-CoV-2 infection.

One-Sentence Summary: We show a unique miRNA and snoRNA profile that is associated with a higher risk of severity in SARS-CoV-2 infected patients.

Introduction

In the beginning of 2020, the World Health Organization (WHO) declared coronavirus disease-2019 (COVID-19) as a global pandemic. The causative organism, severe acute respiratory syndrome coronavirus 2 (SARS-CoV-2), exhibits a wide spectrum of clinical manifestations in disease-ridden patients. Differences in the severity of COVID-19 ranges from asymptomatic infections and mild cases to the severe form, leading to acute respiratory distress syndrome (ARDS) and multiorgan failure with poor survival (1). Moreover, the mortality rate is influenced by ageing, viral strain, pre-existing comorbidities, and the degree of immunocompromise. Indeed, the health and socioeconomic implications of COVID-19 pandemic is enormous, and thus warrants the search of new interventions and treatment measures. Recent research has suggested that a unique non-coding RNA signature can aid in identifying the likelihood of developing specific disease outcomes (2). Alterations of miRNA levels in the blood have been described in multiple inflammatory and infectious diseases, including SARS-related coronaviruses (3–9). MiRNAs are endogenous small non-coding RNAs, around 22 nucleotides, that bind specific messenger RNAs (mRNAs) through complementary base-pairing (10). Hence, miRNAs can regulate various cellular processes, including proliferation, apoptosis, and differentiation, by binding to the 3'UTR of target mRNAs inducing their degradation, thus serving a fundamental role in post-transcriptional repression (11, 12). In this context, a single miRNA can target several genes, and multiple miRNAs may regulate a single gene. Hence, identification of miRNAs as well as characterization of miRNA-mRNA interactions in SARS-CoV-2 infection is important to understand their role in disease pathogenesis, progression, and severity (13–15). Accumulating evidence is also implicating snoRNAs in numerous physiological and pathological processes, including their interaction with some RNA viruses (16, 17). SnoRNAs have been involved in ribosomal RNAs (rRNAs) modification and maturation, including pseudouridylation and 2'-O-methylation, alternative splicing, polyadenylation of genes, and formation of protein complexes with fibrillarin, a component of several ribonucleoproteins (18). There are no reports

yet with a comprehensive characterization of ncRNAs in SARS-CoV-2 infection, therefore, we report for the first time the snoRNA and miRNA signature in the peripheral blood of severe COVID-19 cases (n = 9), as compared to mild (n = 10) and asymptomatic(n = 10) patients. This study analyzed using Affymetrix Genechip miRNA 4.0 array, a total 29 COVID-19 patients that are age and comorbidities matched and were recruited between July and October 2020 in Qatar.

Results

First, we identified differentially expressed miRNAs (DEMIs) and snoRNAs in severe patients as compared to mild and asymptomatic cases, a $|\log_2$ (fold change)| >1.5 and an FDR < 0.2 were used as cutoffs. We found 25 differentially expressed ncRNAs in severe versus asymptomatic, and 50 differentially regulated ncRNAs in severe versus mild cases. Of the 7 ncRNAs that were unique in severe versus asymptomatic, there were 5 upregulated and 2 downregulated transcripts, whereas, of the 32 uniquely differentially expressed ncRNAs in severe versus mild, there were 13 upregulated and 19 downregulated. Interestingly, we also observed 18 ncRNAs that were common in both severe versus mild, and severe versus asymptomatic comparisons (Fig. 1A). Altogether, differential expression (DE) analysis showed a signature of 58 unique ncRNAs that was associated with COVID-19 severity (Fig. 1B **and C**). Notably, the most highly expressed DEMIs/snoRNAs in severe versus asymptomatic are hsa-miR-494-3p, hsa-miR-1246, ACA40, hsa-miR-4532, ACA15. Furthermore, the top 5 DEMIs/snoRNAs in severe versus mild are ACA40, hsa-miR-3609, hsa-miR-6790-5p, hsa-miR-126-3p, hsa-miR-885-3p (**Table. S1** and **S2**). Additionally, we report for the first time 20 differentially expressed snoRNAs, namely ACA15 (SNORA15), ACA18 (SNORA18), ACA20 (SNORA20), ACA40 (SNORA40), ACA57 (SNORA57), ENSG00000206785 (SNORA15C), ENSG00000207062 (SNORA15B-1), ENSG00000212378 (SNORD78), HBII-135, HBII-289, U17b, U29, U44, U59A, U76, U78, and U79 (**Table. S3**). Our novel findings suggest that SARS-CoV-2 infection benefits from gene expression programs regulated by snoRNAs, including C/D box snoRNAs (SNORDs) and H/ACA box snoRNAs. Interestingly, no DEMIs were found in mild versus asymptomatic comparison with the applied cut-offs. These data suggest that both miRNAs and snoRNAs dysregulation is associated with a severe form of COVID-19.

Next, we searched for putative targets for all identified DEMIs in the blood of severely ill COVID-19 patients, and then constructed a network of miRNA targets to reveal pathways and mechanisms underpinning disease severity. To this end, we used the miRTarBase database, which is curated with > 50,000 miRNA-target interactions and validated experimentally by reporter assay, western blot, microarray and next-generation sequencing. In total, we found 2,764 unique validated target genes for the DEMIs. The resulting target genes list was used in functional enrichment analyses to identify top deregulated pathways in severe COVID-19 patients. Remarkably, key enriched KEGG pathways for the 2,764 miRNA-target genes include JAK-STAT, TGF-beta, P53, MAPK, and WNT signaling pathways (Fig. 2). Furthermore, other hallmark gene sets in the Molecular Signatures Database with important biological implications at the top of the list include hypoxia, TNF-alpha signaling via NF-kB, G2-M Checkpoint, and mTORC1 Signaling (**Table. S4**). Interestingly, miRNA-target gene network analysis (MTGN) elucidated 13 nodes of

DEMIs namely hsa-miR-145-5p, hsa-miR-199a-5p, hsa-miR-18a-5p, hsa-miR-126-3p, hsa-miR-98-5p, hsa-let-7g-5p, hsa-miR-494-3p, hsa-let-7f-5p, hsa-miR-139-5p, hsa-let-7i-5p, hsa-miR-1246, hsa-miR-99b-5p, and hsa-miR-572 (Fig. 2). We demonstrate 29 regulated genes targeted by more than 6 DEMIs (**Table. S5**).

The prospect of using blood miRNAs and snoRNAs as biomarkers can be instrumental in identifying patients with higher risk of severity and mortality. In this context, we calculated a correlation matrix to examine individual associations between the identified common (Fig. 3) and unique (**Fig. S1**) DEMIs and snoRNAs in severe cases, and routine laboratory tests such as complete blood count (CBC), glucose, electrolytes, liver and kidney function parameters and inflammatory markers. Several of these clinical markers have been linked to prognosis in COVID-19 patients. We found a significant correlation between several DEMIs and snoRNAs and certain hematological and serological parameters, including WBC count, lymphocyte (%) (Fig. 4A), absolute neutrophil count (Fig. 4B), neutrophil (%), RBC count, hemoglobin, hematocrit, D-Dimer and albumin (**Fig. S2**). These observations can be validated in larger cohorts to help in early detection of patients at higher risk of severity, and thus in selection of dynamic treatment regimens.

Discussion

Interestingly, numerous observed DEMIs in this study have been highlighted in host-pathogen interactions (21). For instance, the family of let-7e/miR-125a/miR-200 miRNAs have been reported to mediated ACE2 gene silencing (22). Likewise, miR-494-3p has been shown to regulate proliferation, invasion, and apoptosis by PTEN/AKT signaling (23). Additionally, impaired B cell function was reported via PTEN-mediated inhibition of the PI3K pathway during viral infections (24). Moreover, the host hsa-miR-494-3p has been reported to promote Enterovirus 71 replication by direct targeting of PTEN (25). Whereases, inhibition of hsa-miR-1246 was demonstrated to reduce the cytotoxicity of Ebola virus glycoprotein in vitro. With multiple viral miRNAs sharing similarities with the host miRNAs, in silico computational studies also uncovered several putative host miRNAs involved in controlling viral replication and limiting disease progression (14, 26–28). These host miRNAs are predicted to bind viral sequences modulating cellular immune responses, metabolic pathways, and inhibiting host miRNA maturation, thus facilitating viral escape. Notably, we found 16 DEMIs targeting CDKN1A, a potent cyclin-dependent kinase inhibitor, also known as p21. Interestingly Ivermectin inhibits p21 activated kinase 1 (PAK1), a serine/threonine kinase with oncogenic activity. Caly et al. reported that ivermectin decreased SARS-CoV-2 RNA viral load in vitro by 5000-fold with a single treatment (19). Another target of multiple DEMIs is Transmembrane protein 135 (TMEM135), which is involved in mitochondrial metabolism and regulating the balance between mitochondrial fusion and fission. Moreover, regulatory component of the cyclin D2-CDK4 complex, which inhibits retinoblastoma protein family and controls the cell-cycle G1/S transition, was also regulated by five different DEMIs detected in severely ill patients. The MTGN analysis suggests that SARS-CoV-2 infection is regulated by a complicated miRNA regulatory network, through multiple miRNAs targeting the same gene, and single miRNAs targeting multiple genes.

Several studies have reported the fundamental role of interferons in COVID-19 disease severity (29). Similarly, the identified miRNA in this study (Fig. 2) suppress interferon signaling via binding interferon target genes. Additionally, multiple viruses, including SARS-CoV-2 haven been reported to enhance TGF-β signaling, which is known to induce fibrosis and suppress adaptive immunity (30). Our data suggests a modulation of TGF-β signaling, via the surface receptors and canonical SMAD and MAPK pathways, regulating adaptive immune responses and tissue repair. These findings are in line with the relative lymphopenia reported in severe COVID-19 (1). Captivatingly, siRNA studies targeting candidate snoRNAs provide an evidence of their functional roles in virus–host interactions against numerous viruses ,while knock-down studies have demonstrated that RNA viruses require specific C/D box snoRNAs for optimal replication (17). Thus, a validated COVID-19 miRNA and snoRNAs signature could be a useful tool to discriminate COVID-19 infections from other respiratory viral infections, identify asymptomatic infections, and develop proteins and metabolite-based tests. This report provides a systematic identification of miRNAs and snoRNAs profile in the blood of SARS-CoV-2 patients with different disease severity, which expands on the previous computational approaches in COVID-19-associated ncRNAs profiling. This study has extended our understanding of the miRNAs and snoRNAs regulatory mechanisms underlying the pathogenesis of SARS-CoV-2 infection, which can be explored further to produce promising therapies.

References

1. G. Chen *et al.*, Clinical and immunological features of severe and moderate coronavirus disease 2019. *J Clin Invest* **130**, 2620–2629 (2020).
2. H. Tang *et al.*, The noncoding and coding transcriptional landscape of the peripheral immune response in patients with COVID-19. *Clin Transl Med* **10**, e200 (2020).
3. R. E. Drury, D. O'Connor, A. J. Pollard, The Clinical Application of MicroRNAs in Infectious Disease. *Front Immunol* **8**, 1182 (2017).
4. S. Fulzele *et al.*, COVID-19 Virulence in Aged Patients Might Be Impacted by the Host Cellular MicroRNAs Abundance/Profile. *Aging Dis* **11**, 509–522 (2020).
5. E. Girardi, P. Lopez, S. Pfeffer, On the Importance of Host MicroRNAs During Viral Infection. *Front Genet* **9**, 439 (2018).
6. D. Gonzalo-Calvo *et al.*, Circulating microRNA profiles predict the severity of COVID-19 in hospitalized patients. *Transl Res*, (2021).
7. H. Henzinger, D. A. Barth, C. Klec, M. Pichler, Non-Coding RNAs and SARS-Related Coronaviruses. *Viruses* **12**, (2020).
8. M. A. Khan, M. R. U. Sany, M. S. Islam, A. Islam, Epigenetic Regulator miRNA Pattern Differences Among SARS-CoV, SARS-CoV-2, and SARS-CoV-2 World-Wide Isolates Delineated the Mystery Behind the Epic Pathogenicity and Distinct Clinical Characteristics of Pandemic COVID-19. *Front Genet* **11**, 765 (2020).
9. H. Shaath, N. M. Alajez, Identification of PBMC-based molecular signature associational with COVID-19 disease severity. *Heliyon* **7**, e06866 (2021).

10. D. P. Bartel, MicroRNAs: genomics, biogenesis, mechanism, and function. *Cell* **116**, 281–297 (2004).
11. M. G. Barbu *et al.*, MicroRNA Involvement in Signaling Pathways During Viral Infection. *Front Cell Dev Biol* **8**, 143 (2020).
12. A. Bernier, S. M. Sagan, The Diverse Roles of microRNAs at the Host(-)Virus Interface. *Viruses* **10**, (2018).
13. C. Hum *et al.*, MicroRNA Mimics or Inhibitors as Antiviral Therapeutic Approaches Against COVID-19. *Drugs* **81**, 517–531 (2021).
14. L. Natarelli *et al.*, MicroRNAs and Long Non-Coding RNAs as Potential Candidates to Target Specific Motifs of SARS-CoV-2. *Noncoding RNA* **7**, (2021).
15. S. Zhang *et al.*, The miRNA: a small but powerful RNA for COVID-19. *Brief Bioinform* **22**, 1137–1149 (2021).
16. R. Hutzinger *et al.*, Expression and processing of a small nucleolar RNA from the Epstein-Barr virus genome. *PLoS Pathog* **5**, e1000547 (2009).
17. S. Stamm, J. S. Lodmell, C/D box snoRNAs in viral infections: RNA viruses use old dogs for new tricks. *Noncoding RNA Res* **4**, 46–53 (2019).
18. T. Bratkovic, J. Bozic, B. Rogelj, Functional diversity of small nucleolar RNAs. *Nucleic Acids Res* **48**, 1627–1651 (2020).
19. L. Caly, J. D. Druce, M. G. Catton, D. A. Jans, K. M. Wagstaff, The FDA-approved drug ivermectin inhibits the replication of SARS-CoV-2 in vitro. *Antiviral Res* **178**, 104787 (2020).
20. T. Alam, L. Lipovich, miRCOVID-19: Potential Targets of Human miRNAs in SARS-CoV-2 for RNA-Based Drug Discovery. *Noncoding RNA* **7**, (2021).
21. R. Marchi *et al.*, The role of microRNAs in modulating SARS-CoV-2 infection in human cells: a systematic review. *Infect Genet Evol* **91**, 104832 (2021).
22. S. Nersisyan, M. Shkurnikov, A. Turchinovich, E. Knyazev, A. Tonevitsky, Integrative analysis of miRNA and mRNA sequencing data reveals potential regulatory mechanisms of ACE2 and TMPRSS2. *PLoS One* **15**, e0235987 (2020).
23. X. T. Li *et al.*, miR-494-3p Regulates Cellular Proliferation, Invasion, Migration, and Apoptosis by PTEN/AKT Signaling in Human Glioblastoma Cells. *Cell Mol Neurobiol* **35**, 679–687 (2015).
24. A. Getahun *et al.*, Impaired B cell function during viral infections due to PTEN-mediated inhibition of the PI3K pathway. *J Exp Med* **214**, 931–941 (2017).
25. Q. Zhao *et al.*, Host MicroRNA hsa-miR-494-3p Promotes EV71 Replication by Directly Targeting PTEN. *Front Cell Infect Microbiol* **8**, 278 (2018).
26. S. Jafarinejad-Farsangi, M. M. Jazi, F. Rostamzadeh, M. Hadizadeh, High affinity of host human microRNAs to SARS-CoV-2 genome: An in silico analysis. *Noncoding RNA Res* **5**, 222–231 (2020).
27. J. B. Pierce *et al.*, Computational Analysis of Targeting SARS-CoV-2, Viral Entry Proteins ACE2 and TMPRSS2, and Interferon Genes by Host MicroRNAs. *Genes (Basel)* **11**, (2020).

28. S. Saini *et al.*, Genome-wide computational prediction of miRNAs in severe acute respiratory syndrome coronavirus 2 (SARS-CoV-2) revealed target genes involved in pulmonary vasculature and antiviral innate immunity. *Mol Biol Res Commun* **9**, 83–91 (2020).
29. Y. M. Kim, E. C. Shin, Type I and III interferon responses in SARS-CoV-2 infection. *Exp Mol Med* **53**, 750–760 (2021).
30. M. Ferreira-Gomes *et al.*, SARS-CoV-2 in severe COVID-19 induces a TGF-beta-dominated chronic immune response that does not target itself. *Nat Commun* **12**, 1961 (2021).

Declarations

Acknowledgments: We gratefully acknowledge Dr Hashim Alhussain for providing support in BSL-3 laboratory at Qatar University.

Funding:

Qatar University QUST-1-CMED-2021-2 (FC)

Author contributions:

Conceptualization: AP, FC, FM

Methodology: AD, AI, AP, IA, RA, RK, SD, FC

Investigation: AD, AI, AP, RK, FC, FM

Visualization: AD, AP, FC, FM

Funding acquisition: FC

Project administration: AA, AE, ALA, EE, FC, ID, MA, MM

Supervision: AE, AP, FC

Writing – original draft: AD, AP, FC, FM

Writing – review & editing: AD, AE, AP, FC, ID, RA

Competing interests: The authors declare that there is no conflict of interest.

Data and materials availability: Additional data and code generated during the current study are available from the corresponding author.

Materials And Methods

Study design and data collection

This research is in accordance with the Reporting of Observational Studies in Epidemiology (STROBE) recommendations, the Code of Ethics of the World Medical Association. This study was granted ethical approval from the Medical Research Center at Hamad Medical Corporation (MRC-05-084, Immunological and immune-genetic investigations in COVID-19 patients with varying disease severity, 06/21/2020). All study participants gave written informed consent where possible, and deferred consent was obtained for ICU cases. Form 173 recruited patients in this prospective cohort study, 29 male age-matched patients were included. All patients were previously diagnosed with COVID-19 using TaqPath COVID-19 Combo Kit (Thermo Fisher Scientific, Waltham, Massachusetts), or Cobas SARS-CoV-2 Test (Roche Diagnostics, Rotkreuz, Switzerland), with a CT value < 30. Additional criterion for selection was age between 35 and 75 years. Participants were grouped into severe, mild and asymptomatic. Classifying severe cases was based on requirement of oxygen support and ICU admission (n=9). Whereas mild patients were identified based on symptoms and positive radiographic findings with pulmonary involvement (n=10). Patients with no clinical presentation were labelled as asymptomatic cases (n=10). In the severe group, three patients died with respiratory failure listed as the primary cause of death. Blood samples were collected in the PaX gene Blood RNA Tubes (Pre Analytix) at the time of diagnosis, prior to isolation, or hospitalization. Routine laboratory tests included complete blood cell counts, electrolytes, glucose, albumin, total protein, C-reactive protein, procalcitonin, IL-6, D-dimers, ferritin, urea, and liver enzymes.

RNA Isolation and Quality Control

Peripheral venous blood (2.5 mL) in PaX gene tubes was inverted 8-10 times to ensure complete mixing with the lysis reagent. Tubes were then stored upright at room temperature for a minimum of 2 hours, before transferring them to freezer at − 80 °C until RNA isolation. The RNA (both total and miRNA) was isolated with a Blood miRNA kit from Qiagen (PreAnalytiX GmBH Hombrechtikon, Switzerland) following the manufacturer’s instructions. The concentrations and purity of the RNA samples were evaluated spectrophotometrically (Nanodrop ND-1000, Thermo, Wilmington, DE USA). The RNA isolation process was validated by analyzing the integrity of several RNAs with the RNA 6000 Nano Chip Kit (Agilent). The presence of the small RNA fraction was confirmed by the Agilent Small RNA Kit (Agilent).

Microarray and data analysis

Affymetrix Genechip miRNA 4.0 array was used following the manufacturer's instructions for miRNA expression analysis. For each sample, 250 ng of RNA was labelled using the FlashTag™ Biotin RNA Labeling Kit (Genisphere, Hatfield, PA, USA). Following this, the labelled RNA was quantified, fractionated, and hybridized to the miRNA microarray with continuous agitation at 60 rpm for 16 h at 48 °C on a GeneChip Hybridization Oven 640. The miRNA microarray chips were then washed and stained using the Genechip Fluidics Station 450 (Affymetrix, Santa Clara, CA, USA). Finally, the miRNA microarray chips were scanned using an Affymetrix GCS 3,000 scanner (Affymetrix, Santa Clara, CA, USA) and the signal

values were evaluated using the Affymetrix® GeneChip™ Command Console software. Raw data were extracted using the Affymetrix data extraction protocol in the Affymetrix GeneChip® Command Console® (AGCC) Software. All statistical analyses including raw data import, annotation, and quality control were conducted with R statistical software (version 4.0.4, R Foundation). R Bioconductor packages “Biobase” and “oligo” were used for the pre-processing of microarray datasets. Raw expression data in CEL files were read using the “affy” module followed by background correction, normalization, and $\log_2$ transformation using Robust Multiarray Average (RMA) method. The differentially expressed transcripts were screened out via the “limma” package. A comparative analysis between different severity groups was carried out using thresholds of $|\log_2 FC|>1.5$ and FDR<0.2. Hierarchical clustering of differentially expressed miRNAs was carried out using “pheatmap” R package. The prediction of miRNA-target genes was performed using “multiMiR” R package filtering with validated databases, including mirecords, mirtarbase and tarbase. The visualization of miRNA-target genes network was built using “MIENTURNET” tool. The database miRTarBase was used with a threshold of 2 for the minimum number of miRNA-target interactions, 1 for the adjusted p-value (FDR), and with filter by evidence categories set to strong. Functional enrichment analysis of target genes list was performed using the “Enrichr” platform including Kyoto Encyclopedia of Genes and Genomes (KEGG) pathway enrichment analysis. Spearman rank correlation tests were calculated to assess the correlation between blood parameters and the levels of DE ncRNAs employing “ggstatsplot” R package. Since all clinical variables had a non-normal distribution, comparisons between different groups of severity were performed using the Kruskal-Wallis rank sum test for continuous variables, and Fisher's Exact Test for categorical. Values were reported as medians and interquartile range [IQR]. Two tailed p-values were calculated and p-value <0.05 was considered statistically significant.

Figures

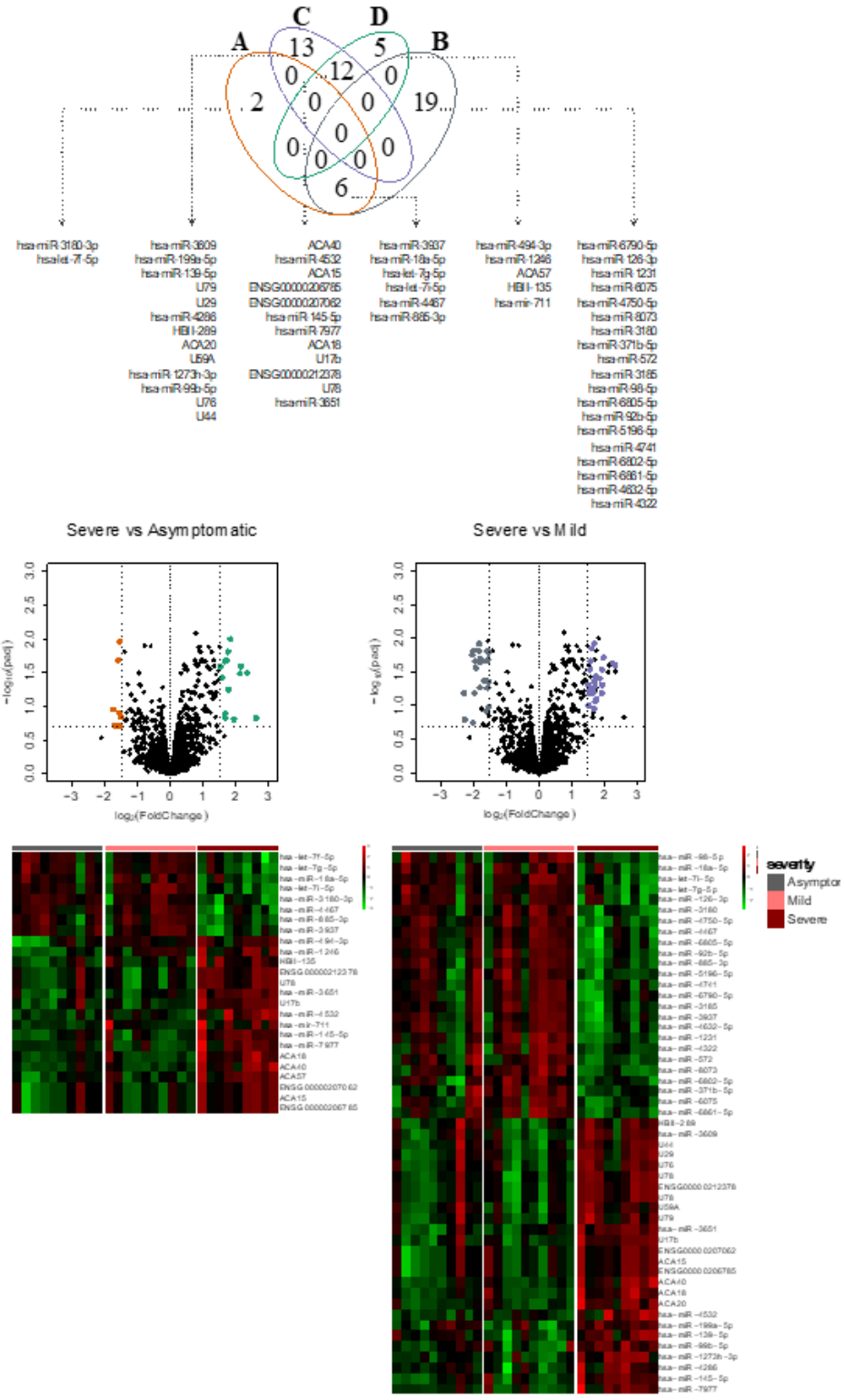

Figure 1

Differential expression analysis of ncRNAs (miRNAs/snoRNAs) in asymptomatic, mild, and severe COVID-19 patients. (A) A Venn diagram of the number of unique and common DEMIs and snoRNAs in severe versus asymptomatic (D: green: upregulated, A: orange: downregulated), and in severe versus mild (C: purple: upregulated, B: grey: downregulated). The overlap of the two ovals in the top of the diagram represents 12 ncRNAs shared between the two upregulated lists, and the two ovals in the bottom of the

diagram represents 6 ncRNAs shared between the two downregulated lists. The areas of no overlap represent the number of uniquely (not shared) ncRNAs in each respective comparison, namely 7 ncRNAs in severe versus asymptomatic, and 32 ncRNAs in severe versus mild comparison. (B) Volcano plots of differentially expressed ncRNAs, with y-axis as - log10 adjusted p-value and x-axis as the log2-fold change. The vertical lines represent a threshold of |log2-fold change| > 1.5, either upregulated (right side) or downregulated (left side), while the horizontal lines represent an FDR < 0.2. Each colored point represents an individual probe in severe versus asymptomatic comparison (D: green: upregulated, A: orange: downregulated), and in severe versus mild comparison (C: purple: upregulated, B: grey: downregulated). (C) Hierarchical clustering of Log2 normalized expression values of the differentially expressed ncRNAs in severe versus asymptomatic comparison (n=25), and in severe versus mild (n= 50).

hsa-miR-145-5p		hsa-miR-199a-5p	hsa-miR-18a-5p	hsa-miR-126-3p	hsa-miR-98-5p	hsa-let-7g-5p	hsa-miR-494-3p	hsa-let-7f-5p	hsa-miR-139-5p	hsa-let-7i-5p	hsa-miR-1246	hsa-miR-99b-5p	hsa-miR-572
SOX2	MTMR14	EZH2	ESR1	SPRED1	E2F1	KRAS	PTEN	IL13	IGF1R	SOCS1	DYRK1A	IGF1R	CDKN1A
CDKN1A	FAM3C	LIF	PTEN	PLK2	HMGA2	COL1A2	CDK6	MPL	CXCR4	IL13	NFIB	ARID3A	
YES1	NIPSNAP1	DDR1	CTGF	HOXA9	MYC	MYC	BCL2L11	CYP19A1	RAP1B	COPS8	GSK3B		
CLINT1	KREMEN1	EDN1	NCOA3	CRK	CASP3	HMGA2	BMI1	COPS8	NFKB1	COPS6			
IRS1	TSPAN8	MAP3K11	NR3C1	VEGFA	NCOA3	IGF2BP1	MYC	GPS1	HRAS	GPS1			
TMOD3	PODXL	HIF1A	HIF1A	VCAM1	EZH2	BCL2L1	TFAM	CCND1	OIP5	IGF1			
HOXA9	APH1A	CD44	TGFBR2	IRS1	IL13	IL13	FOXJ3	COPS6	ACTC1	AGO1			
FSCN1	ABHD17C	SMAD4	SMAD4	SOX2	MPL	BMI1	RAD23B	MYH9	SMARCA4				
MYC	NANOG	CAV1	ATM	TWF1	IL6	AGO1	CXCR4	DYRK2	BCL2				
DFFA	ETS1	SIRT1	NEDD9	DNMT1	PGRMC1	CASP3	BCL2	AGO1	PDE4D				
IGF1R	RREB1	ARHGAP12	DICER1	KRAS	HK2	THBS1	CFTR	IL6					
PPM1D	CD44	CTSC	SMAD3	SLC7A5	NRAS	TGFBR1	IGF1R						
FZD7	SOX9	NFKB1	PIAS3	CRKL	ITGB3	SMAD2	MYH2						
SRGAP1	SMAD3	ACVR1B	BCL2	BCL2	CYP19A1	AKT2	TFPI						
EIF4E	TGFBR2	VEGFA	SMAD2	CXCR4	EDN1	DDR1	AKT1						
VEGFA	CTNND1	CDH2	SDC4	SIRT1	IGF1								
IRS2	SP1	GSK3B	STK4	EZH2	SALL4								
ESR1	CDK6	FZD4	DNMT1	ROCK1	CTNND1								
JAG1	DDX6	JAG1	RUNX1	AKT1	BCL2								
NEDD9	ARF6	HK2	MEF2D										
PAK4	HMGA2	KRAS	TNFAIP3										
NRAS	ROCK1	SMAD3											
ILK	E2F3	ETS1											
CTGF	RPS6KB1	PDE4D											
SOCS7	CFTR	TGFB2											
MDM2	ABCC1	LDLR											
CDH2	FXN	RAB21											
HDAC2	MSH3	PIAS3											
RTKN	TGFB2	ITGA3											
AKR1B10	SMAD2	FZD6											
TPM3	VPS51	TGFBR1											
TMEM9B		SLC27A1											

KEGG Pathway	Number of Genes	Set Number
MAPK Signaling Pathway	187	264
Focal Adhesion	160	197
Regulation of Actin Cytoskeleton	137	211
Endocytosis	128	176
Cell Cycle	127	124
WNT Signaling Pathway	113	149
Ubiquitin Mediated Proteolysis	102	131
Neurotrophin Signaling Pathway	99	125
Chemokine Signaling Pathway	92	184
TGF Beta Signaling Pathway	86	85
P53 Signaling Pathway	85	66
Spliceosome	84	123
Tight Junction	83	128
Adherens Junction	82	68
Insulin Signaling Pathway	81	137
Axon Guidance	79	127
Erbb Signaling Pathway	75	86
Oocyte Meiosis	73	110
JAK STAT Signaling Pathway	72	151

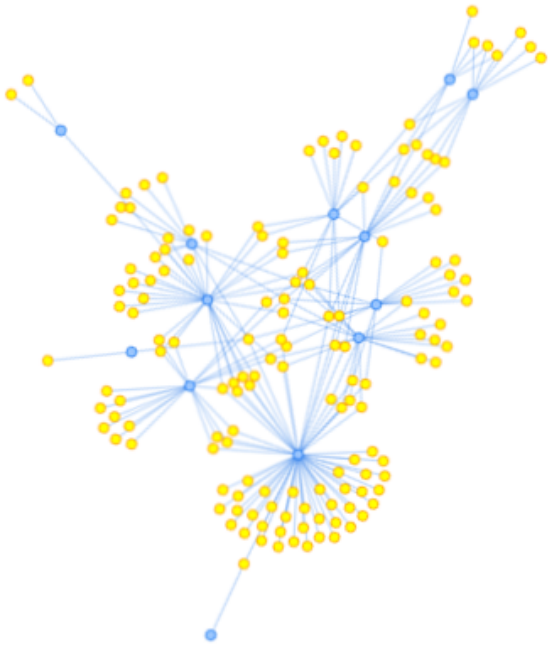

Figure 2

Functional and pathway enrichment analyses using a list of common DEMIs shared by severe versus asymptomatic, and severe versus mild comparisons. Network-based visualization of differentially expressed miRNAs and their associated target genes. The blue nodes represent the miRNA, and the yellow nodes represent its targeted gene. The name of the miRNA is highlighted in red for upregulated, and in green for downregulated, whereases target genes that are highlighted in yellow are those that are

targeted my more than one miRNA. KEGG enrichment analysis is showing the names of deregulated pathways.

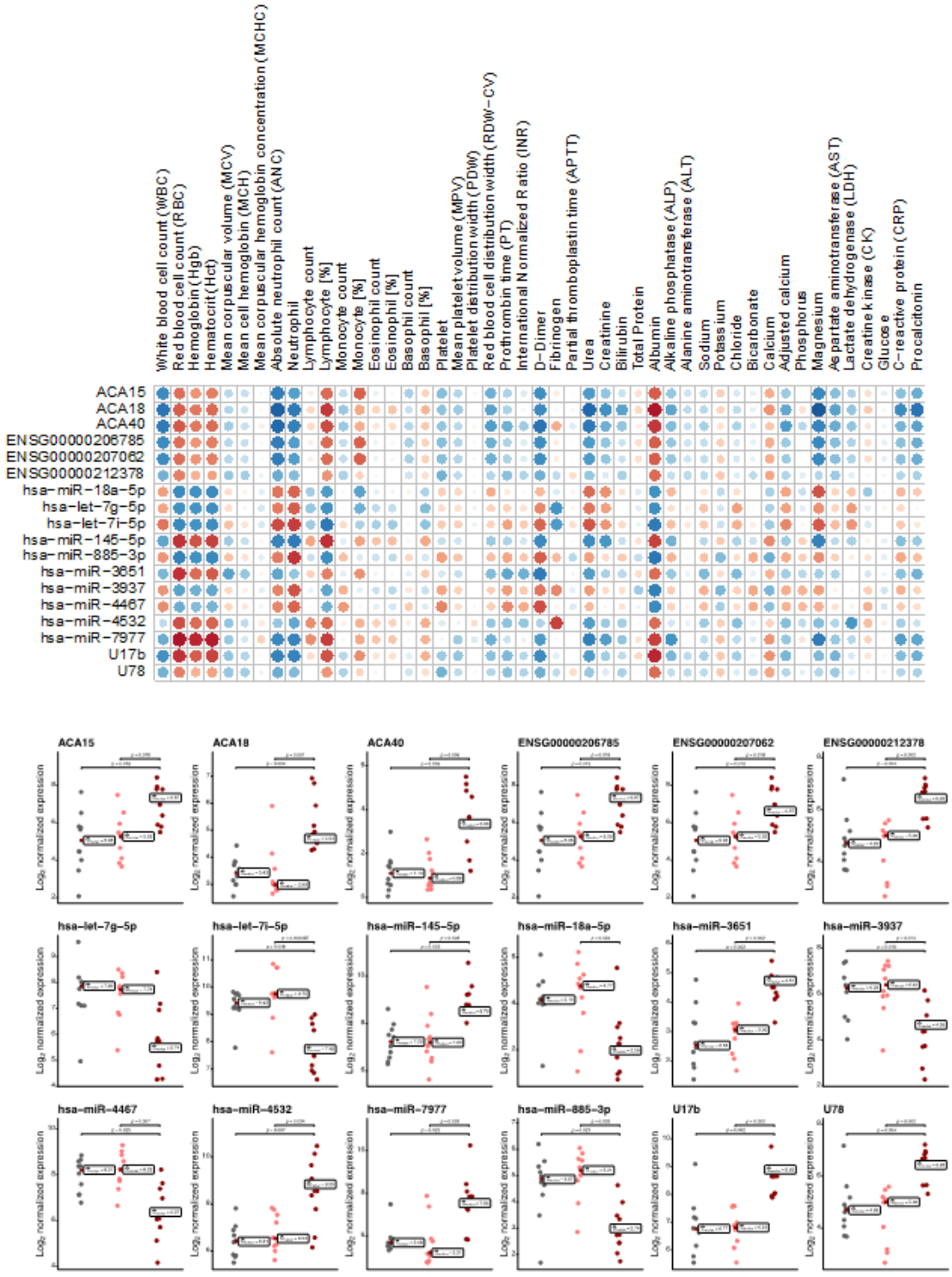

Figure 3

Association of routine clinical markers with differentially expressed common miRNAs and snoRNAs. (A) Scatter plots of Log2 normalized expression values of ncRNAs in asymptomatic (n=10, grey), mild (n=10, light orange), and severe (n=9, red) cases. (B) A correlation matrix of the 18 ncRNAs with severity

associated clinical markers based on the Spearman's rho statistic. Color scale ranges from blue (r = −1) to white (r = 0) to red (r = 1).

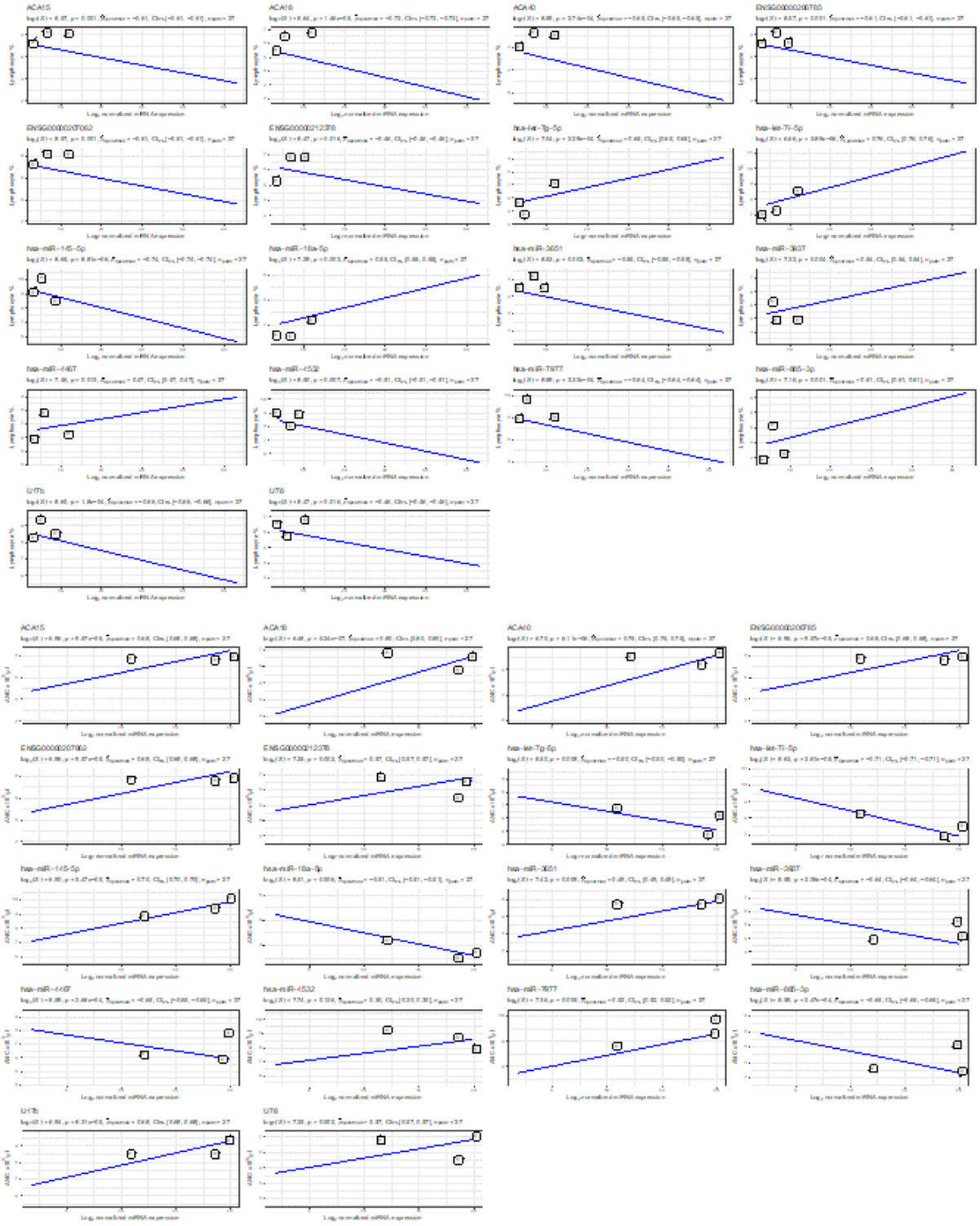

Figure 4

Correlation of lymphocytes (%) and absolute neutrophil count markers with levels of common differentially expressed miRNAs and snoRNAs. Scatter plots x-axis represents Log2 normalized miRNA

expression level, and y-axis as the clinical marker measurement. Each dot represents a single miRNA transcript, and those tagged with D letter show a deceased patient measurement.

Supplementary Files

This is a list of supplementary files associated with this preprint. Click to download.

- SupplementaryncRNAsCOVID19CellDiscovery.docx